



A spherical parameterization approach based on symmetry analysis of triangular meshes*

Jian-ping HU¹, Xiu-ping LIU^{†‡1}, Zhi-xun SU¹, Xi-quan SHI², Feng-shan LIU²

⁽¹⁾School of Mathematical Sciences, Dalian University of Technology, Dalian 116024, China)

⁽²⁾Department of Applied Mathematics and Theoretical Physics, Delaware State University, Dover, DE 19901, USA)

[†]E-mail: xpliu@comgi.com

Received Oct. 19, 2008; Revision accepted Dec. 19, 2008; Crosschecked June 10, 2009

Abstract: We present an efficient spherical parameterization approach aimed at simultaneously reducing area and angle distortions. We generate the final spherical mapping by independently establishing two hemisphere parameterizations. The essence of the approach is to reduce spherical parameterization to a planar problem using symmetry analysis of 3D meshes. Experiments and comparisons were undertaken with various non-trivial 3D models, which revealed that our approach is efficient and robust. In particular, our method produces almost isometric parameterizations for the objects close to the sphere.

Key words: Triangular mesh, Spherical parameterization, Symmetry analysis

doi:10.1631/jzus.A0820728

Document code: A

CLC number: TP391

INTRODUCTION

Mesh parameterization plays a very important role in many mesh processing applications (Sheffer *et al.*, 2006). It involves assigning a position on the parameter domain to each of the mesh vertices, such that the triangles on the parameter domain are not too distorted and do not overlap. Generally, a parameter domain should be homeomorphic to the original mesh. Hence it is best to use a spherical parameter domain for closed genus-zero meshes.

A number of papers have addressed the problem of the construction of spherical parameterizations. It is well known that any closed genus-zero surface can be mapped conformally onto the sphere. Therefore, many previous methods focused on finding angle preserving mappings. Recently, geometry images (Gu

et al., 2002) have emerged as an appealing tool in geometry processing. A spherical surface can be unfolded to form a regular 2D grid (Praun and Hoppe, 2003). Therefore, spherical parameterization can also help create geometry images. However, spherical conformal mapping often lacks control of area distortion, resulting in significant undersampling. The existing non-linear methods (Friedel *et al.*, 2005; Li *et al.*, 2004; Praun and Hoppe, 2003; Zhou *et al.*, 2002; 2004) aimed at solving this problem usually lead to intricate and computationally expensive numerical schemes. Although a linear method was proposed by Zayer *et al.*(2006), a date line connecting two poles must be prescribed beforehand. The choice of the two poles is not obvious and may affect the result, especially for complex geometry surfaces. Consequently, the reduction of both area and angle distortions of spherical parameterization is still a challenging problem.

In this paper, we present a novel approach for solving this problem (Fig.1). The essence of the approach is that spherical parameterization reduces to a 2D planar problem with the help of symmetry

[‡] Corresponding author

* Project supported by the National Natural Science Foundation of China (Nos. 60673006 and 60533060), the Program for New Century Excellent Talents in University (No. NCET-05-0275), China, and the IDeA Network of Biomedical Research Excellence Grant (No. 5P20RR01647206) from National Institutes of Health (NIH), USA

analysis of triangular meshes. With this simplification, we can incorporate the existing quasi-harmonic maps (Zayer *et al.*, 2005a) into our frame to construct low distortion spherical parameterizations. The primary advantages of our algorithm are: (1) Quality: The parameterizations generated by our algorithm have low distortion both in angles and areas. In particular, our approach produces almost isometric parameterizations for the objects close to the sphere; (2) Efficiency: The computation time of our method is dominated only by solving sparse linear systems. In general we can parameterize meshes containing tens of thousands of triangles in a few seconds.

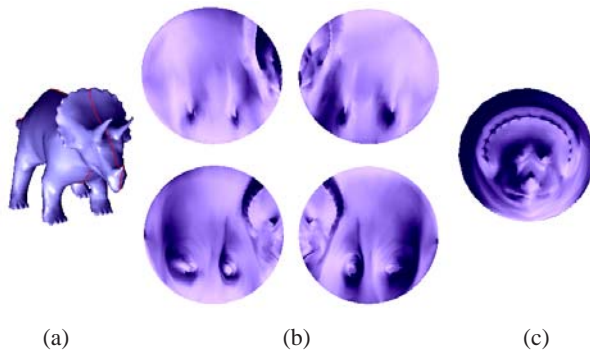


Fig.1 Stages of our approach for the Triceratops model. (a) Split the model into two pieces. The highlighted curve is the cut seam; (b) Establish two hemispherical parameterizations (HMPs) with both low area and angle distortions. Above: two initial HMPs; Below: improvements on the two initial HMPs; (c) Stitch two HMPs together smoothly to generate the final spherical mapping

Motivation and overview

Our work is based on the crucial observation that a sphere has reflective symmetry about any plane through the center; hence the reflective symmetry of spherical parameterization can capture distortion in some sense. The ideal case is that spherical parameterizations should reflect the symmetry of the models completely. Therefore, if we split a closed genus-zero mesh into two pieces with the optimal reflective symmetry, then each piece can be independently parameterized onto the corresponding hemisphere with the lowest distortion. Noting that each piece resulting from the split is topologically equivalent to a disk, and stereographic projection is a bridge between the planar and spherical parameterization, we can construct each hemispherical parameterization (HMP) with low distortion using existing quasi-harmonic map tech-

niques developed for planar parameterization. To generate the final smooth mapping, we stitch the two HMPs together by Laplacian smoothing on the sub-patch around the cut seam.

RELATED WORKS

In the last decade, many studies have been carried out on mesh parameterization (Floater and Hormann, 2005; Sheffer *et al.*, 2006). In the following, we briefly review related works on spherical parameterization in relation to the type of parametric distortion that is minimized.

Early spherical parameterization techniques (Alexa, 2000; Isenburg *et al.*, 2001) attempted to extend the graph embedding method of Tutte (1963) to spheres. They did not preserve any shape properties of the input mesh. Another approach (Shapiro and Tal, 1999), without considering distortion, depended on multi-resolution techniques. It firstly embeds base mesh onto the sphere which is generated by simplifying the original model, and then adds back the vertices progressively.

Many approaches attempt to construct angle preserving spherical mappings (Haker *et al.*, 2000; Gotsman *et al.*, 2003; Sheffer *et al.*, 2003; Gu *et al.*, 2004; Hu *et al.*, 2004; Saba *et al.*, 2005; Kharevych *et al.*, 2006; Li *et al.*, 2006; Liu *et al.*, 2008). Haker *et al.*(2000) generated spherical conformal mappings by lifting the planar angle preserving parameterizations to a sphere through stereographic projection. An elegant theory was proposed by Gotsman *et al.*(2003) extending the planar dirichlet energy to a sphere. Unfortunately, it does not provide an efficient way to solve the resulting quadratic system. Although not mentioned in their research, Gu *et al.*(2004) used projected Gauss-Seidel to solve the nonlinear system. Saba *et al.*(2005) pointed out that the projected Gauss-Seidel iterations decrease the residual for only a finite number of iterations. They proposed a practical method combining projected Gauss-Seidel iteration with nonlinear minimization to obtain the final solution.

To avoid the additional constraints involved in solving the spherical dirichlet energy problem, Friedel *et al.*(2005) modified the discrete energy function accounting for the particularities of the

spherical setting, and blended angle and area measures to control distortion. The approaches of Praun and Hoppe, 2003; Zhou *et al.*, 2002; 2004; Li *et al.*, 2004) related to the goal in this study are based on multi-resolution techniques similar to the method of Shapiro and Tal (1999). Praun and Hoppe (2003) extended the stretch defined in the plane by Sander *et al.*(2001) to a sphere. When progressively adding back the vertices, they used a nonlinear optimization method to minimize the spherical stretch. A linear approach directly aimed at balancing angle and area distortions was proposed by Zayer *et al.*(2006). They firstly cut the mesh along a date line connecting two poles prescribed by the user and computed a conformal mapping in the curvilinear coordinates, then used scalar quasi-harmonic maps to reduce the area distortion.

SPLIT OF MESHES ACCORDING TO SYMMETRY ANALYSIS

The first processing stage in our approach consists of splitting the surface into two disk-like patches. We introduce a novel splitting method based on the optimum reflective symmetry plane of input models. In essence, it is directly related to the technique of symmetry analysis. It has been carefully studied for decades (Mitsumoto *et al.*, 1992) and is still an active research field (Pauly *et al.*, 2008). Symmetry is one of the basic features of many natural and man-made objects, and can be used to guide reconstruction, shape retrieval and classification, mesh segmentation, and so on. Consequently, symmetry analysis plays an important role in computer vision and computational geometry.

Recently, Mitra *et al.*(2006) detected partial and approximate symmetries using a sampling approach to accumulate local evidence of pair wise symmetries in a transformation space. They then used it for shape symmetrization (Mitra *et al.*, 2007). However, their approach focused on finding perfect symmetries of shapes. The objective of our work is to compute the optimum reflective plane for all models (even if they have no perfect reflective symmetries). So we use the reflective symmetry descriptor technique (Kazhdan *et al.*, 2003) of 3D meshes to reach our goal. The descriptor represents a measure of reflective symmetry

for an arbitrary 3D model for all planes through the centroid. We can regard the plane corresponding to the minimum measure as the optimum reflective plane. Given a plane through the centroid, the measure can be computed by the L_2 -difference between the density function f and its reflection $\gamma(f)$, i.e.,

$$SM(f, \gamma) = \|f - \gamma(f)\|,$$

where f is constructed by transforming the 3D model into 3D function sampled on a regular voxel grid. It is defined by

$$f(\mathbf{x}) = \exp(-D^2(\mathbf{x}) / R^2),$$

where $D(\mathbf{x})$ is the Euclidean distance transform, giving the distance from \mathbf{x} to the nearest point on the model M and R is the average distance from a point on M to the centroid. $D(\mathbf{x})$ can be computed by the efficient algorithm of Meijster *et al.*(2000) in the regular voxel grid.

Now we can split the model according to the optimum symmetry plane. As for symmetrical models, the intersection curve between the plane and the models can be regarded as the cut seam (Fig.1a). However, it is not reasonable to use this simple split method for unsymmetrical models. In fact, there are more intersection closed curves for some complex objects. It is evident that a split regarding any of them as the cut seam will destroy the symmetry. Consequently, we propose an alternative way to account for the symmetry of unsymmetrical models (Fig.2). The method depends on the well known Voronoi diagram concept. It can be described briefly as follows:

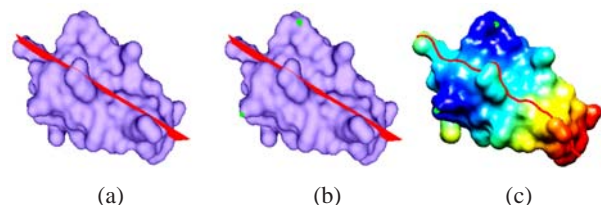


Fig.2 The split of the unsymmetrical Blob model. (a) Extract the optimum symmetry plane; (b) Find the two most symmetrical vertices for the optimum symmetry plane on the mesh model; (c) Generate the Voronoi diagram of the two vertices

(1) Find the two most symmetrical vertices in the mesh for the optimum symmetry plane as the seeds of the Voronoi diagram. For each vertex v of the mesh, we first compute the symmetry point s with respect to the optimum symmetry plane in R^3 . Then we find the closest vertex v^* of s on the mesh using the above Euclidean distance transform. We define a symmetry measure for the two vertices v and v^* as their Euclidean distance. The two vertices corresponding to the minimum measure are chosen as the seeds of the Voronoi diagram.

(2) Use the efficient fast marching method to compute the Voronoi diagram of the two vertices (Kimmel and Sethian, 1999). The Voronoi edge can be regarded as the final cut seam.

The intuition for this method is that it can split a symmetrical object into two symmetrical parts. Accordingly, it accounts for not only the symmetry measure but also the complex structure of unsymmetrical objects.

LOW DISTORTION HMP

Our approach for the construction of low distortion HMP starts from an initial HMP, and then uses quasi-harmonic maps to reduce both area and angle distortions. The key ingredient in this step is how to incorporate the quasi-harmonic maps developed for planar parameterization into our spherical setting.

Initial HMP

The main tools are the most widely known mean value coordinates approach (Floater, 2003) and stereographic projection for the construction of the initial HMP. We first map the boundary vertices of the 3D piece into a 2D convex polygon with vertices on a unit circle. Then we solve a sparse linear system with the following equations about interior vertices:

$$\sum_j w_{ij}(\mathbf{x}_j - \mathbf{x}_i) = 0, \quad i \in \text{interior vertices}, \quad (1)$$

where $\{\mathbf{x}_j\}$ are vertices corresponding to the one ring neighbors of $\{\mathbf{x}_i\}$ in the parameterization, and $\{w_{ij}\}$ are mean value coordinate weights. This computationally simple procedure produces a valid shape preserving planar parameterization.

An initial HMP can be generated by lifting the unit disk parameterization to the hemisphere according to the inverse stereographic projection. Although stereographic projection may produce fold-overs in the discrete case (Sheffer *et al.*, 2006), we can guarantee the objectivity by mapping a unit disk to a hemisphere. It is obvious that for arbitrary triangles in the unit disk, their images on the sphere are always in the same order.

Improvement of the initial HMP

Recently Zayer *et al.* (2005a; 2005b) proposed tensorial quasi-harmonic maps to reduce the distortion of planar parameterization. The essence of the approach is to introduce a piecewise tensor field that locally mimics the Jacobian of the initial map from a given planar configuration to the surface in 3D. It mimics the original 3D shape not only in angles but also in areas as the tensor captures the properties of the Jacobian of the initial map. In effect, it tries to find the most isometric mapping in a least squares sense. In the spherical setting, Zayer *et al.* (2006) pointed out that it is not obvious how to incorporate the Jacobian of the initial spherical mapping into the curvilinear coordinate setting. In our frame, we can easily incorporate the Jacobian of the initial mapping to reduce the distortion.

In fact, the initial HMP can be decomposed into two mappings: One is the stereographic projection s^{-1} from the hemisphere to the unit disk; The other is the mapping g from the unit disk to the piece P (Fig.3). Now, our aim is to construct a quasi-harmonic map f from the unit disk to itself so that $s \circ f$ exactly mimics the behavior of g . The quasi-harmonic map f can be computed by solving the quasi-harmonic equation: $\text{div}(\mathbf{C} \text{grad} f) = 0$, where \mathbf{C} is the Jacobian of f . A direct discretization based on an extension of the mean value coordinates yields the same form equations as Eq.(1) for the interior vertices. w_{ij} is recomputed by the Jacobian tensor \mathbf{C} (Zayer *et al.*, 2005a). The key to the construction of the quasi-harmonic map is the generation of the Jacobian \mathbf{C} .

We now describe how we compute the Jacobian \mathbf{C} in our setting. Let us consider a single triangle T_0 in the piece P (Fig.3). To make the mapping $s \circ f$ mimic the behavior of g , we have the following equation according to a simple computation of their deformations:

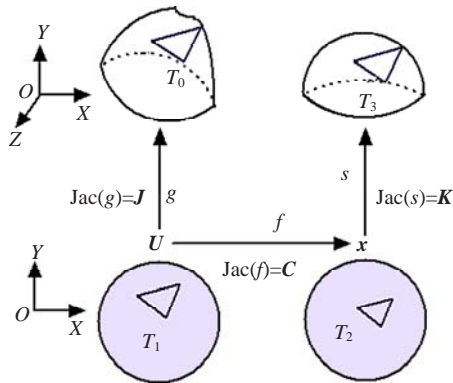


Fig.3 Improvement of the initial HMP

The triangle T_0 is located in the piece P , T_1 and T_2 are both triangles in the unit disk, while the triangle T_3 is on the hemisphere. T_1 corresponds to T_0 under the mapping g , while f maps T_1 to T_2 and s maps T_2 to T_3 . $Jac()$ denotes the Jacobian. U and x are both points in the unit disk

$$dU^T J^T J dU = dU^T (KC)^T (KC) dU.$$

Therefore, the Jacobian C of the new mapping f should satisfy:

$$(KC)^T (KC) = J^T J.$$

Since $J^T J$ and $K^T K$ are both the first fundamental form matrices which are symmetrical positive definite, we can compute their square roots A and B respectively, i.e., $J^T J = AA$, $K^T K = BB$. Then we get $C = B^{-1}A$.

The matrix A can be computed by the initial HMP. Noting that stereographic projection is a conformal mapping, we can compute B by $K^T K = \tau I = BB$, where I is the unit matrix and τ is the scalar factor, i.e., the triangle area ratio between the triangles T_3 and T_2 . But unfortunately, the triangle T_2 is unknown. We use the triangle area ratio between T_3 and T_1 as an alternative and derive satisfactory results. This is not surprising since the singular values of the Jacobian of the stereographic projection s vary from 1 to 2 in the unit disk. The variation between T_1 and T_2 for each iteration will not result in an obvious change in the scale factor τ .

Our HMP can be further improved by iteratively resolving the same form sparse linear system Eq.(1) until convergence. In our implement, three to five iterations were used which appeared to be sufficient.

SMOOTHING AROUND THE CUT SEAM

In previous sections, we have described how to

generate two HMPs that are low both in angle and area distortions. The two HMPs are combined by the common boundary. However, it is clear from Fig.4 that some distortions have been caused near the cut seam. To reduce such distortions, we define a sub-patch around the cut seam by choosing its five ring neighborhoods, then perform Laplacian smoothing on the sub-patch (similar to Zayer *et al.*(2006)). Although the Laplacian smoothing is designed to reduce only angle distortion, the area distortion does not increase too much in our setting as the sub-patch has low area distortion before smoothing. To avoid fold-overs, we restrict the new vertex inside its kernel on the sphere. The smoothing is repeated until a fixed number of iterations are reached. Generally, five iterations give good results (Fig.4).

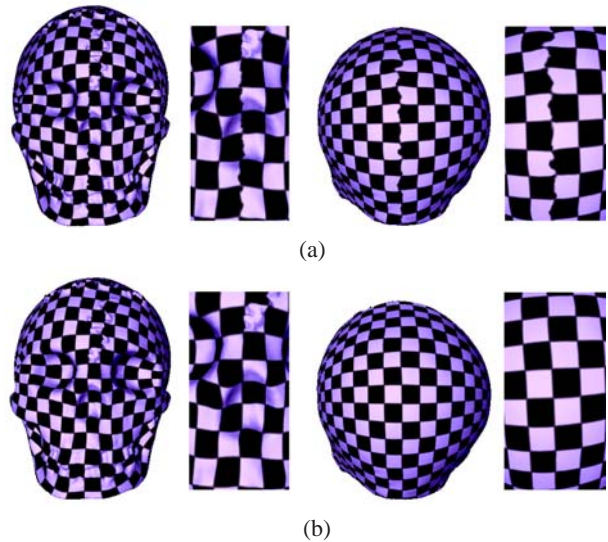


Fig.4 Texture mapping effect of Laplacian smoothing applied to the Skull model. (a) Before smoothing; (b) After smoothing. The comparison of the zoom-in near the cut seam shows that the two HMPs are well stitched

RESULTS AND DISCUSSION

We implemented the above algorithm on a 3.2 GHz PC with 2 G RAM. To solve a linear system, we used the backslash operator of Matlab version 7.2. The size of the test models varied from 5660 to 149 524 triangles. The split step took between 1.5 and 3.6 s. The runtime for solving the sparse linear systems was in the order of a few seconds. In the final smoothing step, the time varied from 0.05 to 0.8 s. Table 1 summarizes the total runtime of our approach.

Table 1 Performance comparison of different methods

Model	Triangles	Method	Angle distortion	Area distortion	Time (s)
Skull (Fig.7)	40000	Ours	0.12	0.07	6.9
		Zayer	0.21	0.10	4.7
		Saba	0.16	0.52	115.6
Hygeia (Fig.7)	53736	Ours	0.11	0.10	8.8
		Zayer	0.17	0.12	6.9
		Saba	0.18	0.38	160.1
Gargoyle (Fig.7)	20000	Ours	0.39	0.46	4.4
		Zayer	0.41	0.52	2.6
		Saba	0.32	1.09	92.1
Manbody (Fig.7)	35998	Ours	0.54	0.82	6.5
		Zayer	0.58	0.87	4.3
		Saba	0.26	1.38	198.0
Bimba (Fig.8)	149524	Ours	0.29	0.32	27.9
		Saba	0.23	1.02	1425.9
Bunny (Fig.9)	69666	Ours	0.23	0.28	11.9
		Zayer	0.27	0.41	9.3

Zayer: the method of Zayer et al.(2006); Saba: the method of Saba et al.(2005)

To evaluate the visual quality of a spherical parameterization, we used the parameterization to map the normals of the original model to the sphere, and to map a spherical chessboard texture (Fig.5a) to the original model. A spherical chessboard texture can be generated by mapping a regular quadrilateral chessboard to a sphere according to polar coordinates. For a quantitative evaluation of a spherical parameterization we determined the area and angle distortions as follows:

$$Dist_{area} = \sum_i \left| \frac{A(T_i)}{\sum_{T_j \in M} A(T_j)} - \frac{A(T_i^*)}{\sum_{T_j^* \in M^*} A(T_j^*)} \right|,$$

$$Dist_{angle} = \frac{1}{3F} \sum_i \sum_{j=1}^3 |\theta_{ij} - \theta_{ij}^*|,$$

where $Dist_{area}$ is taken over all the triangles T_i and

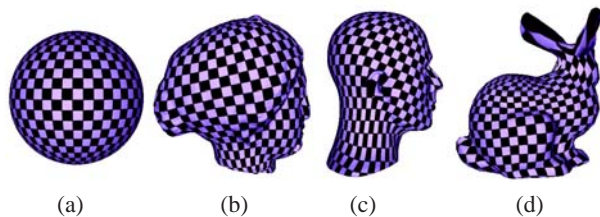


Fig.5 Texture mapping results of our method. (a) Spherical chessboard texture; (b) Hygeia model; (c) Mannequin model; (d) Bunny model

T_i^* of the original mesh M and the parameterization M^* , respectively, $Dist_{angle}$ is taken over all the angles θ_{ij} and θ_{ij}^* of the triangles of M and M^* , respectively, F is the total number of triangles of M , and $A()$ denotes the triangle area.

All the results (Fig.1, Figs.4~9, Table 1) demonstrated that our approach has low distortion both in angles and areas. In particular, our work produces almost isometric parameterizations for the objects close to the sphere (Fig.7: Skull and Hygeia). Furthermore, the resulting solutions are valid in that they have no triangle fold-overs. Currently, we cannot claim that properties of our approach have any general validity. The main reason is that the weight w_{ij} generated by a general tensor matrix C is not always positive when improving two HMPs using the quasi-harmonic maps. But because the positivity of weights about convex combination maps is only a sufficient condition and given the good properties of quasi-harmonic maps (Zayer et al., 2005a), general validity is quite likely. Fig.6 shows the parameterization sensitivity for two chosen seeds for the unsymmetrical Blob model using our method. It can be seen that parameterization using the split of the Voronoi diagram of the two most symmetrical points has lower distortion.

We compared our method to the practical approach of Saba et al.(2005) (Figs.7 and 8, Table 1), which aims to solve the minimizing problem of the spring dirichlet energy using a nonlinear optimized method on the sphere. For complex objects, their results have lower angle distortion while our results clearly have lower area distortion (Fig.7: Gargoyle and Manbody, Fig.8). We believe that these results arise from the fact that the isometric spherical maps exist only for objects with similar shapes to the

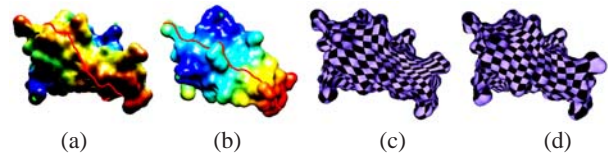


Fig.6 The parameterization sensitivity for two seed choices for the unsymmetrical Blob model using our method. (a) One is a random point; the other is its furthest point on the mesh; (b) The two most symmetrical points; (c) Texture mapping corresponding to (a). Angle distortion 0.31, area distortion 0.23; (d) Texture mapping corresponding to (b). Angle distortion 0.19, area distortion 0.22



Fig.7 Parameterization comparison. (a) The original models. From top: Skull, Hygeia, Gargoyle and Manbody; (b) The method of Saba *et al.*(2005); (c) The method of Zayer *et al.*(2006); (d) Our method

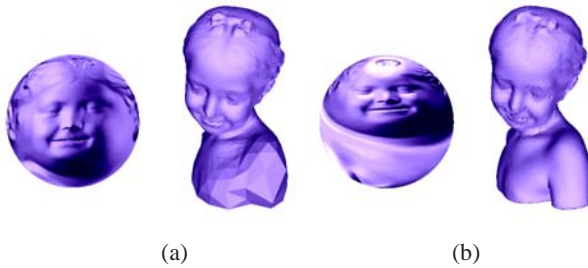


Fig.8 Parameterization and remeshing comparison for the Bimba model. (a) The method of Saba *et al.*(2005). In the remeshing result, one shoulder has been under-sampled; (b) Our method



Fig.9 Parameterization and remeshing comparison for the Bimba model. (a) The method of Zayer *et al.*(2006). In the remeshing result, the two ears have been under-sampled; (b) Our method

sphere, while the conformal spherical maps exist for any closed genus-zero objects.

We also compared our approach to a linear method aimed at balancing angle and area distortions (Zayer *et al.*, 2006) (Figs.7 and 9, Table 1). As mentioned above, the choice of two poles in their method is not obvious. An additional advantage of our approach is that the cut seam generated by the optimal symmetry plane provides a good guideline for the selection of the date line. However, it is hard to quantify because the approach is sensitive to this choice as illustrated in Fig.10. In all test objects, we note that with careful choice of two poles on the cut seam their method often produces good results. But even so, our results still have lower distortion than theirs both in angles and areas. We believe the reason is that our method improves the spherical mapping using quasi-harmonic maps incorporating the Jacobian of the initial mapping.



Fig.10 Parameterization comparison for different date lines of Zayer *et al.*(2006). (a) Angle distortion 0.38, area distortion 0.43; (b) Angle distortion 0.41, area distortion 0.51

Our low area and angle distortion spherical parameterizations can be used to create geometry images and can also be used to create remeshed geometry. We considered remeshing using subdivision connectivity triangulations since it is both a convenient way to illustrate the properties of a parameterization and an important subject. We have developed two remeshing strategies (Fig.11). One is to map a nearly uniform icosahedron subdivision at different levels on the sphere back to an object surface. The other is to construct an adaptive subdivision remeshing of the icosahedron on the sphere according to the guaranteed error bound in order to keep the number of triangles small and avoid the overhead of subdividing the mesh to a fine level. Figs.8 and 9 show the comparison between our approach and some state of the art methods using the same uniform remeshing strategy (the uniform subdivision level is 5). Our results produced a much better remeshed geometry,

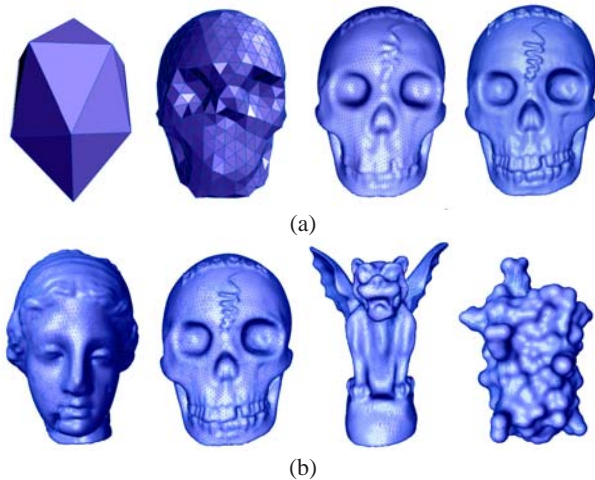


Fig.11 Remeshing results by our parameterizations. (a) The uniform remeshing results of the Skull model at the 0, 3rd, 5th, 6th subdivision level of the icosahedron on the sphere; (b) The adaptive remeshing results of the icosahedron on the sphere for different models (from left: Hygeia, Skull, Gargoyle, and Blob) with the guaranteed error bound (0.005). The error bound has been normalized by the bounding box diagonals of the models

while the methods of Saba *et al.*(2005) and Zayer *et al.*(2006) led to some undersampling.

CONCLUSION


Given a closed genus-zero triangular mesh, we have presented an efficient spherical parameterization approach aimed at simultaneously reducing area and angle distortions. According to symmetry analysis, the low distortion spherical parameterization is generated by the independent construction of two HMPs. The time of our approach is dominated only by solving sparse linear systems. Experiments and comparisons reveal that our approach is robust and efficient.

It is important to note that our method is heuristic and is supported by numerical results. Currently we are not able to support it by rigorous mathematical theories.

References

- Alexa, M., 2000. Merging polyhedral shapes with scattered features. *The Vis. Comput.*, **16**(1):26-37. [doi:10.1007/PL00007211]
- Floater, M.S., 2003. Mean value coordinates. *Comput. Aided Geometric Des.*, **20**(1):19-27. [doi:10.1016/S0167-8396(03)00002-5]
- Floater, M.S., Hormann, K., 2005. Surface Parameterization: a Tutorial and Survey. Dodgson, N.A., Floater, M.S., Sabin, M.A. (Eds.), *Advances in Multiresolution for Geometric Modeling*. Springer-Verlag, Heidelberg, p.157-186. [doi:10.1007/3-540-26808-1_9]
- Friedel, I., Schröder, P., Desbrun, M., 2005. Unconstrained Spherical Parameterization. *ACM SIGGRAPH Technical Sketches*, ACM, New York, USA. [doi:10.1145/1187112.1187274]
- Gotsman, C., Gu, X., Sheffer, A., 2003. Fundamentals of Spherical Parameterization for 3D Meshes. *Computer Graphics Proc., Annual Conf. Series*, ACM, New York, USA, p.358-364. [doi:10.1145/882262.882276]
- Gu, X., Gortler, S.J., Hoppe, H., 2002. Geometry Images. *Proc. 29th Annual Conf. on Computer Graphics and Interactive Techniques*, ACM, New York, USA, p.355-361.
- Gu, X., Wang, Y., Chan, T.F., Thompson, P.M., Yau, S.T., 2004. Genus zero surface conformal mapping and its application to brain surface mapping. *IEEE Trans. Med. Imaging*, **23**(8):949-958. [doi:10.1109/TMI.2004.831226]
- Haker, S., Angenent, S., Tannenbaum, S., Kikinis, R., Sapiro, G., Halle, M., 2000. Conformal surface parameterization for texture mapping. *IEEE TVCG*, **6**(2):181-189. [doi:10.1109/2945.856998]
- Hu, G., Fang, X., Peng, Q., 2004. Convex combination spherical parameterization. *J. Comput. Aided Des. Comput. Graph.*, **16**(5):632-637 (in Chinese).
- Isenburg, M., Gumhold, S., Gotsman, C., 2001. Connectivity Shapes. *Proc. Conf. on Visualization*. IEEE Computer Society, Washington, D.C., USA, p.135-142.
- Kazhdan, M., Chazelle, B., Dobkin, D., Funkhouser, T., Rusinkiewicz, S., 2003. A reflective symmetry descriptor for 3D models. *Algorithmica: Special Issue*, **38**(1):201-225. [doi:10.1007/s00453-003-1050-5]
- Kharevych, L., Springborn, B., Schröder, P., 2006. Discrete conformal mappings via circle patterns. *ACM Trans. Graph.*, **25**(2):412-438. [doi:10.1145/1138450.1138461]
- Kimmel, R., Sethian, J.A., 1999. Fast Voronoi Diagrams and Offsets on Triangulated Surfaces. *Proc. AFA Conf. on Curves and Surfaces*. Vanderbilt University Press, Nashville, TN, p.193-202.
- Li, L., Zhang, D., Pan, Z., Shi, J., Zhou, K., Ye, K., 2004. Watermarking 3D mesh by spherical parameterization. *Comput. Graph.*, **28**(6):981-989. [doi:10.1016/j.cag.2004.08.002]
- Li, Y., Yang, Z.W., Deng, J.S., 2006. Spherical parameterization of genus-zero meshes by minimizing discrete harmonic energy. *J. Zhejiang Univ. Sci. A*, **7**(9):1589-1595. [doi:10.1631/jzus.2006.A1589]
- Liu, X., Hu, J., Su, Z., Shi, X., 2008. Uniform quasi-conformal spherical parameterization. *J. Comput. Aided Des. Comput. Graph.*, **20**(5):618-624 (in Chinese).
- Meijster, A., Roerdink, J.B.T.M., Hesselink, W.H., 2000. A General Algorithm for Computing Distance Transforms in Linear Time. Goutsias, J., Vincent, L., Bloomberg, D.S. (Eds.), *Mathematical Morphology and Its Applications to Image and Signal Processing*, Kluwer, Boston, p.331-340.

- Mitra, N.J., Guibas, L.J., Pauly, M., 2006. Partial and approximate symmetry detection for 3D geometry. *ACM Trans. Graph.*, **25**(3):560-568. [doi:10.1145/1179352.1141924]
- Mitra, N.J., Guibas, L.J., Pauly, M., 2007. Symmetrization. *ACM Trans. Graph.*, **26**(3), Article No. 63.
- Mitsumoto, H., Tamura, S., Okazaki, K., Kajimi, N., Fukui, Y., 1992. 3D Reconstruction using mirror images based on a plane symmetry recovery method. *IEEE Trans. Pattern Anal. Mach. Intell.*, **14**(9):941-946. [doi:10.1109/34.161352]
- Pauly, M., Mitra, N.J., Wallner, J., Pottmann, H., Guibas, L.J., 2008. Discovering structural regularity in 3D geometry. *ACM Trans. Graph.*, **27**(3), Article No. 43. [doi:10.1145/1360612.1360642]
- Praun, E., Hoppe, H., 2003. Spherical Parameterization and Remeshing. *Computer Graphics Proc., Annual Conf.*, ACM, New York, USA, p.340-350. [doi:10.1145/882262.882274]
- Saba, S., Yavneh, I., Gotsman, C., Sheffer, A., 2005. Practical Spherical Embedding of Manifold Triangle Meshes. *Proc. Int. Conf. on Shape Modeling and Applications*, IEEE Computer Society, Washington, D.C., USA, p.258-267. [doi:10.1109/SMI.2005.32]
- Sander, P., Snyder, J., Gortler, S., Hoppe, H., 2001. Texture Mapping Progressive Meshes. *ACM SIGGRAPH*. New York, USA, p.409-416. [doi:10.1145/383259.383307]
- Shapiro, A., Tal, A., 1999. Polyhedron realization for shape transformation. *The Vis. Comput.*, **14**(8-9):429-444.
- Sheffer, A., Gotsman, C., Dyn, N., 2003. Robust spherical parameterization of triangular meshes. *Comput.*, **72**(1-2):185-193. [doi:10.1007/s00607-004-0056-9]
- Sheffer, A., Praun, E., Rose, K., 2006. Mesh parameterization methods and their applications. *Comput. Graph. Vision*, **2**(2):105-171. [doi:10.1561/0600000011]
- Tutte, W.T., 1963. How to draw a graph. *London Math. Soc.*, **13**(1):743-768. [doi:10.1112/plms/s3-13.1.743]
- Zayer, R., Rössl, C., Seidel, H.P., 2005a. Discrete Tensorial Quasi-harmonic Maps. *Shape Modeling Int. Proc.*, Cambridge, MA, USA, p.276-285. [doi:10.1109/SMI.2005.17]
- Zayer, R., Rössl, C., Seidel, H.P., 2005b. Setting the Boundary Free: A Composite Approach to Surface Parameterization. *Proc. 3rd Eurographics Symp. on Geometry Processing*, Eurographics Association Aire-la-Ville, Switzerland, p.101-110.
- Zayer, R., Rössl, C., Seidel, H.P., 2006. Curvilinear Spherical Parameterization. *Proc. Shape Modeling and Applications*. IEEE Computer Society, Washington, D.C., USA, p.57-64. [doi:10.1109/SMI.2006.9]
- Zhou, K., Bao, H., Shi, J., 2002. A unified framework for digital geometry processing. *Chin. J. Comput.*, **25**(9):904-909 (in Chinese).
- Zhou, K., Bao, H., Shi, J., 2004. 3D surface filtering using spherical harmonics. *Computer-Aided Des.*, **36**(4):363-375. [doi:10.1016/S0010-4485(03)00098-8]



Editor-in-Chief: Wei YANG
 ISSN 1673-565X (Print); ISSN 1862-1775 (Online), monthly

Journal of Zhejiang University

SCIENCE A

www.zju.edu.cn/jzus; www.springerlink.com
jzus@zju.edu.cn

JZUS-A focuses on "Applied Physics & Engineering"
 Online submission: <http://www.editorialmanager.com/zusa/>

JZUS-A has been covered by SCI-E since 2007

➤ **Welcome Your Contributions to JZUS-A**
Journal of Zhejiang University SCIENCE A warmly and sincerely welcomes scientists all over the world to contribute Reviews, Articles and Science Letters focused on **Applied Physics & Engineering**. Especially, Science Letters (3~4 pages) would be published as soon as about 30 days (Note: detailed research articles can still be published in the professional journals in the future after Science Letters is published by *JZUS-A*).